



Minerva Access is the Institutional Repository of The University of Melbourne

Author/s:

Wang, LY;Stuart-Fox, D;Lee, KH;Black, J;Franklin, AM

Title:

A new ultrafast movement enables escape at low temperature

Date:

2025-12-01

Citation:

Wang, L. Y., Stuart-Fox, D., Lee, K. H., Black, J. & Franklin, A. M. (2025). A new ultrafast movement enables escape at low temperature. *Communications Biology*, 8 (1), pp.229-.  
<https://doi.org/10.1038/s42003-025-07650-7>.

Persistent Link:

<https://hdl.handle.net/11343/359882>

License:

[CC BY-NC-ND](#)

<https://doi.org/10.1038/s42003-025-07650-7>

# A new ultrafast movement enables escape at low temperature

Lu-Yi Wang<sup>1</sup> ✉, Devi Stuart-Fox<sup>1</sup>, Ko-Huan Lee<sup>2,3</sup>, Jay Black<sup>4</sup> & Amanda M. Franklin<sup>1</sup>

Escape is a life critical defensive behaviour. One potential escape strategy is using ultrafast movements to relocate quickly. These movements do not rely solely on muscle activation and are beneficial for ectotherms at low temperatures when muscle performance is constrained. However, the functional significance of ultrafast motions is often assumed. Here, we show with high-speed videos that *Astraeus* jewel beetles (Buprestidae) rapidly open their elytra to flick themselves into the air and the movement is of comparable speed to other known ultrafast movements. Our calculations indicate that it is likely a power-amplified mechanism. Behavioural trials and thermal imaging demonstrate that *Astraeus* beetles can flick at >15°C lower body temperatures than walking or flying, suggesting that the behaviour could provide a significant survival advantage at low ambient temperatures. Taken together, we reveal a novel ultrafast movement and show its potential functional value in escape.

Animals have evolved myriad strategies to escape predators and improve survival. While some strategies reduce the probability of detection (e.g., camouflage<sup>1</sup>, hiding in refuges<sup>2</sup>), others reduce the probability of attack after detection (e.g., chemical deterrents<sup>3</sup>, physical armour<sup>4</sup>, playing dead<sup>3</sup>). A common escape strategy once detected is for prey animals to attempt to outrun and outmanoeuvre the predator<sup>5,6</sup>. However, this strategy is unavailable to ectothermic animals at cool ambient temperatures because muscle performance is temperature-dependent. Instead, some ectotherms may use power-amplification systems that produce ultrafast movements with minimal muscle activation, e.g., ref. 7. These systems could overcome the temperature constraint on muscle performance and enable rapid escape at low temperatures, but we lack supporting empirical evidence for this intriguing and potentially widespread escape strategy.

Many organisms achieve high-speed movements by using a power amplification mechanism to circumvent the force-velocity trade-off of muscle motors<sup>8</sup>. This mechanism enables the organism to store elastic energy and instantaneously release energy to help them move more quickly than by muscle control alone<sup>8–10</sup>. Power amplification mechanisms have been identified across the tree of life, including fungi, plants and animals with the mechanism varying among organisms. For example, mantis shrimp use internal latches and an exoskeleton spring to generate powerful strikes with their raptorial appendages to smash snail shells<sup>11</sup>, and fungi powered by a sudden reduction in surface tension triggered by the fuse of two drops discharge ballistospores to disperse<sup>12</sup>. Ultrafast movements are used for a wide range of functions from predation to dispersal and defence. However, most of studies on ultrafast movements have focused on the biomechanics and engineering applications in robotics e.g., refs. 13–15,

while the functional significance of these power amplified systems is usually assumed rather than tested empirically e.g., refs. 9,16.

*Astraeus* jewel beetles (Coleoptera: Buprestidae) are the only genus (55 species) of beetle known to flick themselves upward by rapidly opening the elytra (Fig. 1; Supplementary Movie 1–5; compared with Supplementary Movie 6 showing pre-flight elytra opening). When the elytra open, they rotate instantaneously over the head followed by oscillating back and forth several times. Such behaviour differs in opening angle, speed, and effect (flicking the whole beetle up) from the elytral movements observed in other beetles for pre-flight opening<sup>17</sup>, righting<sup>18</sup>, ultrafast jumping<sup>19,20</sup>, or clicking<sup>21</sup>. It is suggested to be an escape behaviour, allowing the beetle to rapidly relocate themselves when threatened<sup>22,23</sup> and can also be used for righting (see Supplementary Movie 3). The movement occurs in a fraction of a second and can propel the beetle multiple body lengths into the air, indicating that the flick is a power amplified movement. If the motion is power amplified, this may enable the beetles to escape predators at lower body temperatures than that required for other escape behaviours such as flight. In general, escape via muscle activation (e.g., flight) requires beetles to be at active body temperatures above ~25°C depending on their size<sup>24</sup>, whereas pre-loaded elastic energy could be released at much lower body temperatures. Such an escape strategy would be very beneficial at dawn and dusk when their primary predators, birds, are most active but ambient temperatures are cooler. To our knowledge, there are no experimental tests of the hypothesis that power amplification mechanisms enable escape from predators at low ambient temperatures.

In this study, we detail the biomechanics and experimentally test the potential function in escape of the flicking motion in two species of *Astraeus*

<sup>1</sup>School of Biosciences, The University of Melbourne, Melbourne, VIC, Australia. <sup>2</sup>School of Natural Sciences, Macquarie University, Sydney, NSW, Australia.

<sup>3</sup>Health and Biosecurity, Commonwealth Scientific and Industrial Research Organisation (CSIRO), Canberra, ACT, Australia. <sup>4</sup>School of Geography, Earth and Atmospheric Sciences, The University of Melbourne, Melbourne, VIC, Australia. ✉e-mail: [luyi.wang@unimelb.edu.au](mailto:luyi.wang@unimelb.edu.au); [luyiwangtw@gmail.com](mailto:luyiwangtw@gmail.com)

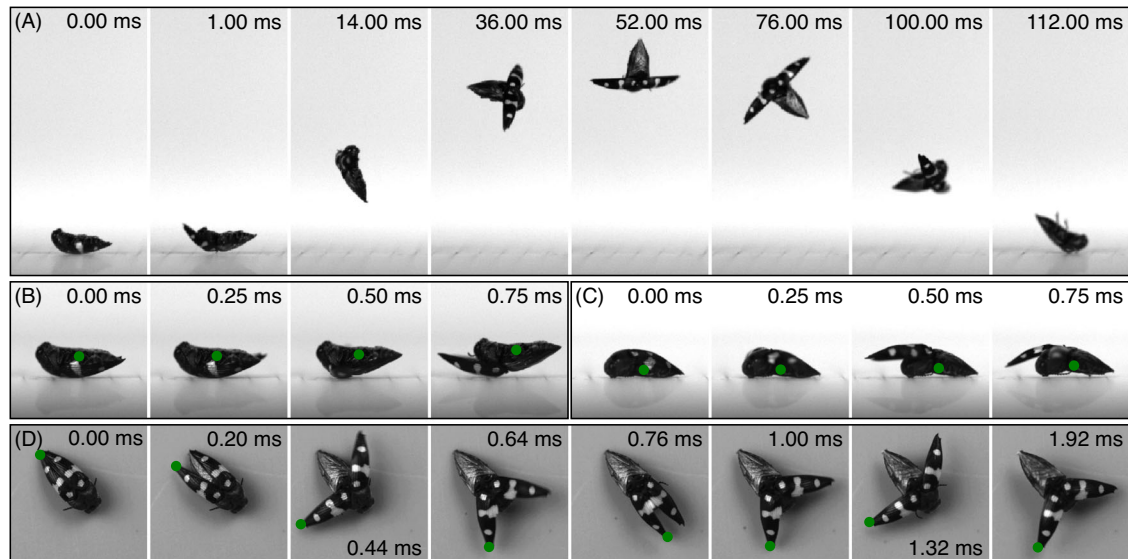


**Fig. 1 | The flicking behaviour in *Astraeus pygmaeus*.** **A** Lateral view of the body projection phase. Lateral view of elytra opening phase from **(B)** upside down and **(C)** right-side up positions and from the top view **(D)**. Green dots in **(B–D)** indicate the points that we used for calculating kinematics of the movements.

jewel beetles. Two species were examined to investigate differences between species that varied in size (small *A. pygmaeus*, mean body length 5.83 mm; large *A. dilutipes*, 8.16 mm). To characterise the kinematics, we filmed the motion using a high-speed camera and we investigated morphology and potential flick-associated structures using micro-CT and electron microscopy. We also conducted behavioural trials combined with thermal imaging, which showed the potential of this ultrafast movement as an escape strategy at low temperatures when the beetles are too cold to fly. Taken together, these results demonstrate a previously undescribed ultrafast movement and its potential function, with an underlying mechanism promising for bioinspired robotic design.

## Results and discussion

### *Astraeus* jewel beetle flick is one of the fastest biological movements

From high-speed videos, we found that the flick comprises two phases: first the elytra (hardened forewings) open extremely quickly and second the beetle is propelled into the air (Fig. 1; Supplementary Movie 1–4; Method: High-speed video recording). Remarkably, beetles can flick from upside down (ventral side up) and right-side up (ventral side down) positions, and this does not have a significant effect on the kinematics of the elytra opening (duration, angular velocity, angular acceleration and force: all  $p > 0.05$ ; number of individuals,  $N = 36$ , number of observations,  $n = 132$ ; Supplementary Table 1–3; see Methods: Kinematics of the elytra opening phase). Thus, the movement does not depend on the elytra contacting a substrate.

During the first phase, the elytra open asynchronously, with the second elytron opening on average 56% faster in angular velocity (*A. pygmaeus*: 1<sup>st</sup>,  $5.51 \pm 1.09 \times 10^3 \text{ rad s}^{-1}$ , 2<sup>nd</sup>,  $8.59 \pm 1.89 \times 10^3 \text{ rad s}^{-1}$ ; mean  $\pm$  SD;  $\chi^2 = 302.83$ ,  $df = 1$ ,  $p < 0.001$ ,  $N = 36$ ,  $n = 132$ ; Supplementary Fig. 1, Supplementary Table 1 and 4) and with 31% higher angular acceleration (*A. pygmaeus*: 1<sup>st</sup>,  $3.27 \pm 0.89 \times 10^7 \text{ rad s}^{-2}$ , 2<sup>nd</sup>,  $4.78 \pm 1.32 \times 10^7 \text{ rad s}^{-2}$ ;  $\chi^2 = 40.44$ ,  $df = 1$ ,  $p < 0.001$ ,  $N = 36$ ,  $n = 132$ ). This movement is extremely fast and amongst the fastest biological movements currently recorded<sup>8,16,25</sup>. To compare with other documented fast movements in nature, we converted the angular velocity and acceleration to linear velocity and acceleration (see Methods: Kinematics of the elytra opening phase). The average peak linear velocity (*A. pygmaeus*, 2<sup>nd</sup> elytron:  $40.49 \pm 7.96 \text{ m s}^{-1}$ ) and linear acceleration (*A. pygmaeus*, 2<sup>nd</sup> elytron:  $2.01 \pm 0.59 \times 10^5 \text{ m s}^{-2}$ ) of elytra tips during elytra opening are comparable with appendage strikes of mantis shrimps ( $31 \text{ m s}^{-1}$ <sup>26</sup>) but are slightly slower than other appendage movements in terrestrial animals of similar size, such as trap-jaw ants ( $64 \text{ ms}^{-1}$ <sup>27</sup>; Fig. 2). The movement differs

from pre-flight elytra opening in *Astraeus* and other beetle species. Ladybird beetles rapidly open their elytra prior to flight at a speed of  $66 \text{ rad s}^{-1}$  and the elytra displacement is roughly 10 degrees from the closed position. Pre-flight elytra opening in *Astraeus* is similar to this movement in ladybirds (Supplementary Movie 6). By contrast, the *Astraeus* beetles' flick is two orders of magnitude faster than that of the ladybird and the elytra rotate to above the head ( $>90$ -degree displacement angle).

During the body projection phase, beetles flicked a vertical height of  $17.53 \pm 12.23 \text{ mm}$  ( $n = 59$ ; Supplementary Fig. 2; Supplementary Table 4; see Methods: Kinematics of the body projection phase) when placed flat on the substrate, with a maximum height of 65 mm recorded in *A. dilutipes*. Beetles in upside down position flicked 92% higher ( $\chi^2 = 17.26$ ,  $df = 1$ ,  $p < 0.001$ ;  $N = 31$ ,  $n = 59$ ; Supplementary Table 1) and 51% faster ( $\chi^2 = 38.83$ ,  $df = 1$ ,  $p < 0.001$ ;  $N = 31$ ,  $n = 59$ ) on average than in right-side up position during the initial take-off. This ability to flick more quickly and to a greater height from an up-side-down position suggests that the movement could be an effective secondary escape strategy, for example if the beetle falls off the leaf after a failed predator attack. The airborne beetle rotated during the ballistic movement with the rotation direction depending on the take-off position, and movement was mostly vertical with limited horizontal displacement. The body projection of *Astraeus* beetles was not as fast as most biological fast movements, including other potential escape behaviours such as invertebrate jumps (Fig. 3; *A. pygmaeus*, upside down position  $1.34 \pm 0.28 \text{ m s}^{-1}$  ( $n = 15$ ) vs. froghopper  $4.7 \text{ m s}^{-1}$ <sup>28</sup>). However, the acceleration of the body (*A. pygmaeus*, upside down position,  $6.53 \pm 2.62 \times 10^3 \text{ ms}^{-2}$ ) was higher than most jumping systems, such as locust jumps ( $1.8 \times 10^2 \text{ m s}^{-2}$ ; Supplementary Fig. 3), which enables them to lift their body off the substrate quickly.

### Flicking kinematics of the two *Astraeus* species

The kinematic performance of *Astraeus* flicks varies between species, which could be owing to differences in size, anatomy, behaviour or physiology. Both mathematical models and comparative analyses indicate that for spring-driven movements of small organisms, acceleration, and maximal power are enhanced with decreasing size even within one order of magnitude<sup>24</sup>. Similarly, the comparative analysis in McHenry, et al<sup>26</sup>, empirically demonstrated that larger mantis shrimp strike more slowly than smaller mantis shrimp, independent of species and raptorial appendage type (smasher or spearer). These align with our results where the smaller *A. pygmaeus* flicks the elytra open at 53% higher angular velocity (Fig. 2C; *A. pygmaeus*,  $7.05 \pm 2.18 \times 10^3 \text{ rad ms}^{-1}$ ,  $N = 18$ ,  $n = 66$ ;

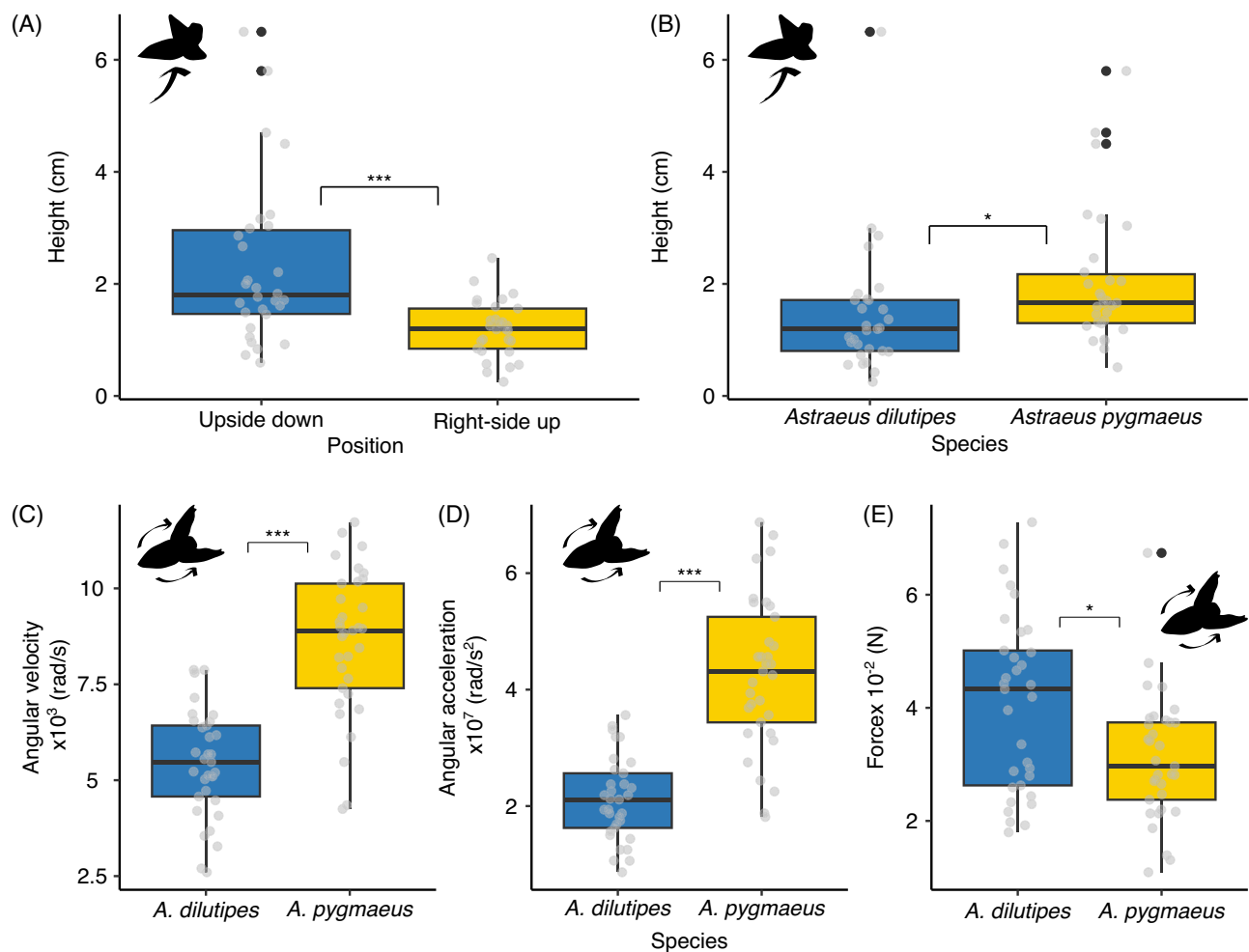


**Fig. 2 | Kinematics of flicking behaviour of *Astraeus dilutipes* and *A. pygmaeus*.** Boxplots show the height of the flicks (A) at different positions (species pooled; Number of individuals,  $N = 31$ , number of observations,  $n = 59$ ) and (B) in difference species (position pooled;  $N = 31$ ,  $n = 59$ ) during body projection. C–E shows the angular velocity, angular acceleration, and force of the second elytron generated

during elytra opening in the two species (position pooled;  $N = 36$ ,  $n = 132$ ). \*\*\* $p < 0.001$  and \* $p < 0.05$ . Data has been pooled to display key results, full results in Supplementary Fig. 1 and 2. Boxes represent the mean, upper quartile and lower quartile, whiskers show 1.5 times the interquartile range, and black dots show outliers. Grey dots are raw data points.

*A. dilutipes*,  $4.60 \pm 1.46 \times 10^3 \text{ rad ms}^{-1}$ ,  $N = 18$ ,  $n = 66$ ;  $\chi^2 = 36.11$ ,  $df = 1$ ,  $p < 0.001$ ,  $N = 36$ ,  $n = 132$ ) with 95% higher angular acceleration (Fig. 2D; *A. pygmaeus*,  $3.78 \pm 1.23 \times 10^7 \text{ rad s}^{-2}$ ,  $N = 18$ ,  $n = 66$ ; *A. dilutipes*,  $1.94 \pm 0.65 \times 10^7 \text{ rad s}^{-2}$ ,  $N = 18$ ,  $n = 66$ ;  $\chi^2 = 54.54$ ,  $df = 1$ ,  $p < 0.001$ ,  $N = 36$ ,  $n = 132$ ) than the larger *A. dilutipes*. The differences in angular velocity and angular acceleration between the two elytra (1<sup>st</sup> vs. 2<sup>nd</sup>) were also significantly greater in the smaller *A. pygmaeus* than the larger *A. dilutipes* (order  $\times$  species; angular velocity,  $\chi^2 = 27.16$ ,  $df = 1$ ,  $p < 0.001$ ,  $N = 36$ ,  $n = 132$ ; angular acceleration,  $\chi^2 = 9.21$ ,  $df = 1$ ,  $p < 0.001$ ,  $N = 36$ ,  $n = 132$ ; Supplementary Fig. 1). By contrast, the larger *A. dilutipes* generated 38% stronger force (Fig. 2E;  $37.75 \pm 15.52 \text{ mN}$ ;  $\chi^2 = 7.82$ ,  $df = 1$ ,  $p < 0.05$ ,  $N = 36$ ,  $n = 132$ ) than the smaller *A. pygmaeus* ( $27.40 \pm 10.29 \text{ mN}$ ) likely due to larger elytron size.

For the body projection phase, *A. pygmaeus* flicked 5.50 mm (or 37%) higher than *A. dilutipes* on average (*A. pygmaeus*:  $20.24 \pm 12.13 \text{ mm}$ ,  $N = 15$ ,  $n = 30$ , *A. dilutipes*:  $14.74 \pm 11.89 \text{ mm}$ ,  $N = 16$ ,  $n = 29$ ; Fig. 2B;  $\chi^2 = 4.03$ ,  $df = 1$ ,  $p < 0.05$ ,  $N = 31$ ,  $n = 59$ ; Supplementary Fig. 2; Supplementary Table 2, 3, 5), but there was no difference in velocity ( $\chi^2 = 1.76$ ,  $df = 1$ ,  $p = 0.18$ ,  $N = 31$ ,  $n = 59$ ) and acceleration ( $\chi^2 = 0.31$ ,  $df = 1$ ,  $p = 0.58$ ,  $N = 31$ ,  $n = 59$ ) between the two species. This isometric difference is also found in the jumps of click beetles where size does not predict the maximum velocity and height<sup>29</sup>. The height of the *Astraeus* flicks is affected by multiple factors such as the contact angle with the substrate, velocity, orientation during the

airborne phase, and air resistance which is associated with cross-section area. These factors might explain the difference in height between the two species of different sizes. Additional to the difference in kinematics performance, our observations of behaviour when caught in insect nets suggest a difference in flicking tendency, where *A. pygmaeus* seems to flick more often than *A. dilutipes*. There are 55 species of *Astraeus* beetles that vary in size (5–17 mm) and behaviour, and therefore offer a promising system to investigate variation in kinematic performance and how it relates to behaviour.

### Flicking requires power amplification

Ultrafast movements are often achieved by power amplification, where the elastic energy is ready-stored and released instantaneously, rather than by muscles alone. Muscles can only output a certain amount of power, and the highest known mass specific power output for any muscle is  $200 \text{ W kg}^{-1}$ <sup>10</sup> (bird flight muscle). Mass-specific power output of the system can be calculated by dividing the maximum power generated by the mass of muscles involved. If the system's mass-specific power output is higher than  $200 \text{ W kg}^{-1}$ , it is likely power amplified. We calculated the maximum mass-specific power of *A. pygmaeus* to be  $1.8 \times 10^5 \text{ W kg}^{-1}$  (see Methods: Test for power amplification), which is substantially higher than the highest known value for muscle and comparable with the most powerful known movements including frog hopper jumps ( $3.6 \times 10^4 \text{ W kg}^{-1}$ ) and predatory strikes

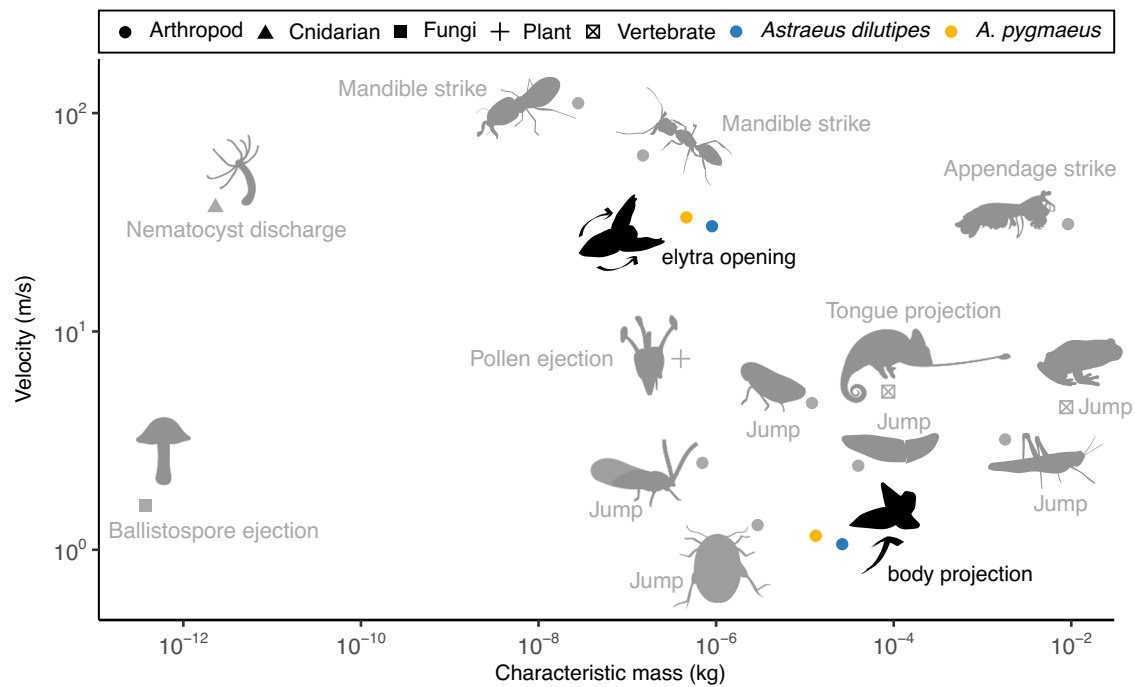


**Fig. 3 | Comparison in maximum velocity between *Astraeus* jewel beetles and fast movements of other biological systems.** Icons indicate termite, trap-jaw ant, hydra, mantis shrimp, bunchberry dogweed stamen, chameleon, froghopper, frog, locust, plant louse, click beetle, fungi, and marsh beetle. Characteristic mass indicates the mass of the projectile or the body part that is displaced during the movement. Data

points of click beetle on the figure are derived from Evans<sup>25</sup>, that of termite from Kuan, et al.<sup>16</sup>, that of marsh beetle from Nadein, et al.<sup>7</sup>, and the rest other than *Astraeus* beetles are derived from Table 2 in Ilton, et al.<sup>8</sup>. Blue dots represent *Astraeus dilutipes* and yellow dots are *A. pygmaeus*. For comparison in acceleration, please see Supplementary Fig. 3.

of mantis shrimp ( $4.7 \times 10^5 \text{ W kg}^{-1}$ )<sup>9,11</sup>. Such high power density indicates that the elytra opening of *Astraeus* beetles is not generated by muscles directly but is a power amplified movement.

To amplify power, small animals often use latch-mediated spring actuation (LaMSA<sup>10</sup>) mechanisms. This mechanism stores energy generated by motors (e.g., muscles) in a spring, which is latched prior release<sup>10</sup>. Upon release of the latch, the energy is released in a short timeframe that generates greater power output than muscles alone and could help animals move more quickly<sup>10</sup>. In beetles, for example, marsh beetles use a LaMSA mechanism in their legs to rapidly jump, enabling them to relocate or escape predators. They store energy in a resilin-bearing extensor ligament, which is latched by the conical tibial projection inserting into the socket at the tibial base, and release the energy to generate ultrafast jumps by contracting the flexor muscle which pulls the projection out of the socket<sup>7</sup>. Alternatively, LaMSA jumping mechanisms may not involve legs, such as the jumping motion observed in click beetles. In click beetles, the energy is latched by two cuticular protrusions (peg and mesosternal lip) resisting against each other at the joint of the prothorax and mesothorax on the ventral side. The jumps are initiated when the peg quickly slides into the cavity behind the mesosternal lip, which causes the beetle body to jack-knife and flick into the air<sup>21</sup>. *Astraeus* beetles seem to have a similar pre-actuation position to click beetles, where the back arches, and the antennae and legs are withdrawn against the body<sup>25</sup> (Supplementary Movie 6). However, arching of *Astraeus* beetles is barely noticeable compared to click beetles (Supplementary Movie 7). Moreover, the peg and mesosternal lip in click beetles are external and easily seen with the naked eye. By contrast, we did not observe any mesosternal lip-like structure and cavity in *Astraeus* beetles from micro-CT data (Fig. 4). Therefore, *Astraeus* beetles likely have a different actuation mechanism from that of click beetles.

Instead, the flick of *Astraeus* beetles likely originates from the release of an internal latch, which is probably associated with the anterior part of the elytra. When one elytron was completely removed or the posterior half of both elytra were removed, the beetle could still flick upwards (Supplementary Movie 8 and 9). However, when both elytra were removed, the

beetle still flexed the body but no flick occurred (Supplementary Movie 10). Additionally, the body projection is likely not due to physical contact between the elytra and substrate. When we placed the beetle in the right-side up position on a tiny platform where any physical contact with the elytra was eliminated, the beetle still flicked (Supplementary Movie 11). Barker<sup>22</sup> proposed that the mechanism of flicking in *Astraeus* beetles was a latch and spring mechanism involving a curved lip on the anterior side of the elytra fitting over the opposite curved projections on the mesothorax. We compared the relative positions of these candidate structures from scanning electron microscope images and micro-CT scans (Fig. 4; Supplementary Fig. 4; see Methods: Structure examination). Based on these data, we do not find support for Barker's proposal because the structures do not slot together. We investigated other structures at the anterior base of the elytra including the scutellum, root of the elytra, and the scutellar lever arms (Fig. 4). These structures may be involved in the elytra opening. Compared to other Buprestid beetles, the scutellum is modified into a point, and both the scutellum and scutellar lever arms rotate together dorsally during elytra opening (Supplementary Fig. 5). It is also possible that the beetle projection could be partly related to the sudden expansion of the body in the dorsal-ventral direction. Exoskeleton deformation can be involved in LaMSA mechanisms<sup>11,30,31</sup> and, while subtle, this expansion could act like the release of a compressed coil. Further mathematical modelling and anatomical studies are required to determine the precise nature and location of the spring and latch.

### Flicking enables escape at low ambient temperature

Ultrafast movements have a wide range of functions in living organisms, including locomotion<sup>9</sup>, predation<sup>11</sup> and dispersal<sup>12,32</sup>. We hypothesised that the flicks may allow jewel beetles to escape predators at low temperatures when the beetles are too cold to fly. To test this hypothesis, we conducted behavioural assays that we videoed using a thermal camera to measure the temperature at which the beetles could voluntarily walk, flick, and fly, and the lowest temperature the beetles can be triggered to flick (see Methods: Escape temperature experiment). We found that *A. pygmaeus* flew at much

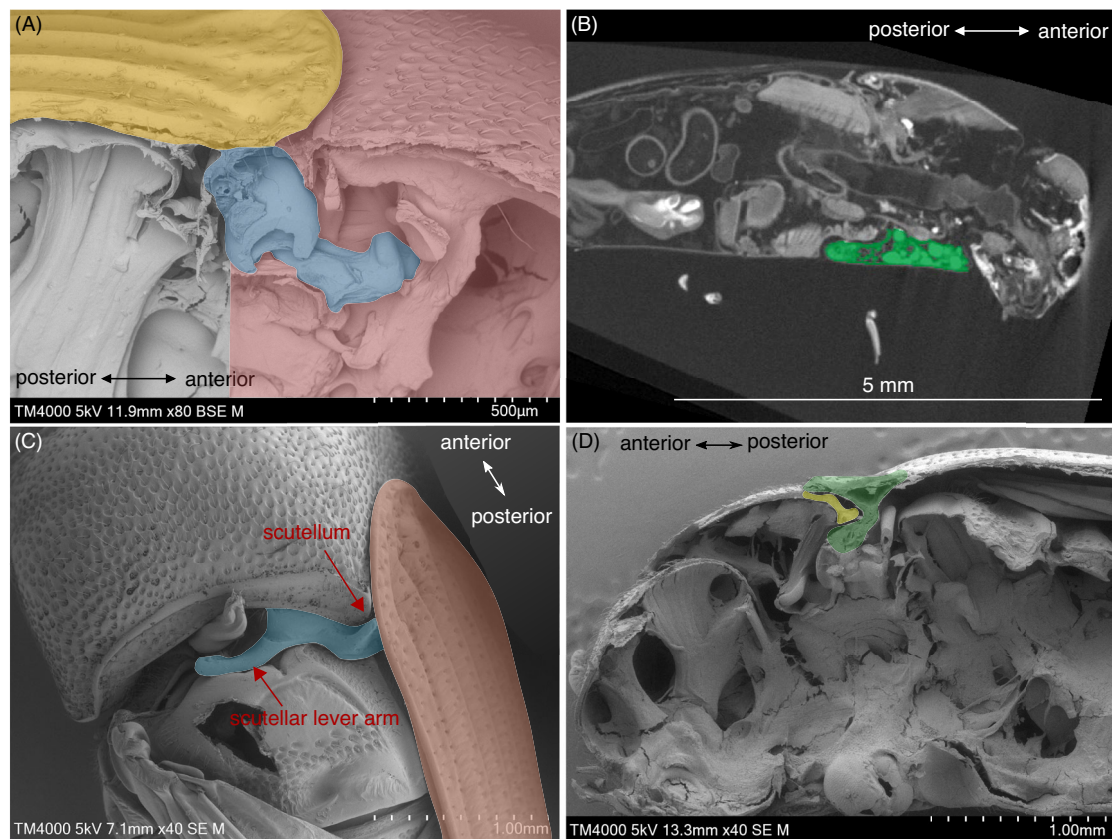


**Fig. 4 | SEM and micro-CT images of potential flick-associated structures in *Astraeus pygmaeus*.** **A** The SEM image of the elytron base of *A. pygmaeus*. Yellow shows the elytron, blue shows the root of the elytron that sits inside the prothorax in red. **B** The micro-CT image shows the cross-section of *A. dilutipes* at elytra closed position with the peg in green. No mesosternal lip or cavity were observed,

suggesting a different mechanism to click beetles. **C** shows the relative positions of the scutellum and scutellar lever arms in blue when elytra are closed. **D** shows the structure suggested by Barker<sup>22</sup> involving a curved lip on the anterior underside of each elytron (green) fitting over the curve on the mesothorax (yellow).

higher body temperature ( $37 \pm 2^\circ\text{C}$ ) than it walked ( $30 \pm 2^\circ\text{C}$ ;  $\chi^2 = 522.27$ ,  $df = 3$ ,  $p < 0.001$ ; post-hoc test,  $p < 0.001$ ,  $N = 35$ ,  $n = 66$ ) or flicked ( $29 \pm 4^\circ\text{C}$ ; post-hoc test,  $p < 0.001$ ) and they walked and flicked at similar body temperature ( $p = 0.69$ ; Fig. 5; Supplementary Table 6). However, when triggered, *A. pygmaeus* was capable of flicking at  $14 \pm 1^\circ\text{C}$ , which is  $15^\circ\text{C}$  less than both voluntary walking and voluntary flicking (both  $p < 0.001$ ). These results confirm that flicking can enable escape when beetles are too cold to fly.

The beetles are largely inactive at dawn and dusk when their potential avian predators are most active<sup>33</sup>. At these times of day, the temperatures are generally much lower and, as poikilotherms, *Astraeus* beetles are not warm enough to fly away when threatened. In Supplementary Movie 12 and 13, we showed that when pinched by forceps, the flicking motion causes the beetles to slide through the forceps and project themselves horizontally. This might be similar to a bird's beak pinching the beetle from both sides. Ultrafast flicking not only enables initial escape, but makes it extremely difficult to track where the beetle lands. The landing site is unpredictable, particularly when the flick's trajectory is altered by the elytra hitting an object in its path. Like click beetles, *Astraeus* beetles do not have the ability to control the landing site and position<sup>34,35</sup>. However, this may be unimportant for escape and flicking could be used to right themselves when they fall to the ground.

## Conclusion

This study provides the first detailed observation, visualisation, and assessment of the kinematics and adaptive value of *Astraeus* beetle flicks. We show that *Astraeus* beetles flick themselves by opening the elytra instantaneously and our calculations indicate that the extremely fast opening of the elytra is power amplified and likely uses a mechanism that

has not been observed in other biological systems. These flicks likely function to escape predators when the ambient temperature is too low to escape by flying away, and probably also function for self-righting when they fall to the ground which is one jewel beetles' predator-avoidance tactics. Ultrafast movements in biological systems have inspired numerous robotic designs in engineering systems such as a locust-inspired jumping robot<sup>13</sup> and chameleon tongue-inspired projector<sup>14</sup>. Among the biomimetic jumping robots, many are inspired by insect jumps via legs<sup>8</sup> while our results here introduce a different locomotion system – flicking open the elytra. Elucidation of the underlying mechanism of the flicking behaviour in *Astraeus* jewel beetles may open exciting avenues for energy-efficient three-dimensional locomotion.

## Methods

### Study system

*Astraeus* is a genus of jewel beetles (Coleoptera: Buprestidae) distributed in Australia, New Guinea, and New Caledonia with >90% of the species (50 out of total 55) endemic to Australia<sup>36</sup>. *Astraeus* beetles are mostly found on their host plants, *Casuarina* and *Allocasuarina* (Casuarinaceae)<sup>36</sup>. *Astraeus dilutipes* and *A. pygmaeus* were chosen as models because both species display flicking behaviour and are reliably abundant, but they differ in body size (*A. dilutipes* c.a. 2.3 mm (40%) longer than *A. pygmaeus* in body length). We collected 24 *A. dilutipes* and 69 *A. pygmaeus* in Marsden Park, New South Wales in November and December 2021, and Licola, Victoria in January 2022 by canopy sweeping their host plants with insect nets. We kept the beetles at  $4^\circ\text{C}$  in the lab and recorded the flicking behaviour within 10 days after capture. The beetles were warmed up to room temperature ( $\sim 25^\circ\text{C}$ ) before the recording.

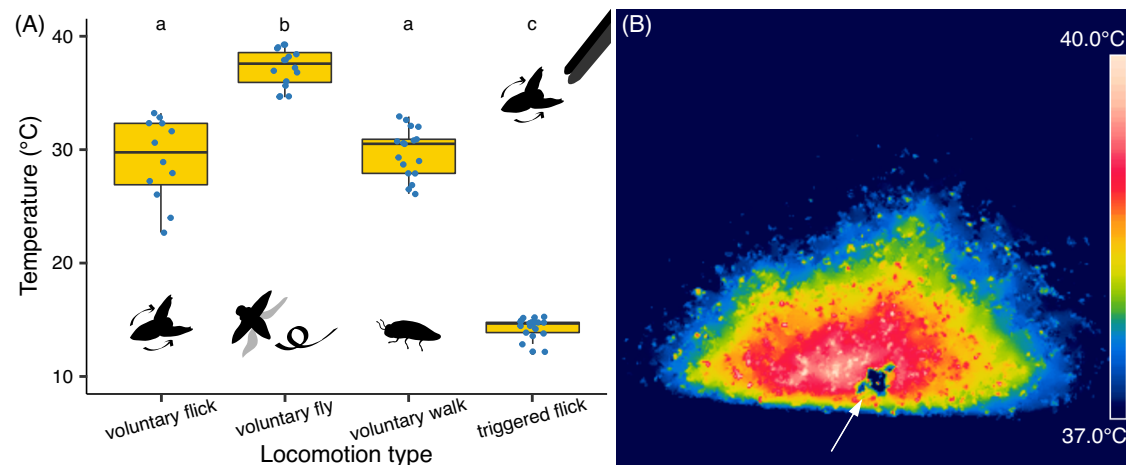


**Fig. 5 | Thermal experiment of the locomotion movements.** **A** Boxplots show the body temperatures at the start of flicking, flying, and walking in *Astraeus pygmaeus*. Bold lines box edges present the means, upper and lower quartiles, respectively with whiskers showing 1.5 times of interquartile range. Blue dots shows raw data

points. Different letters on the top of boxes indicate significant differences ( $p < 0.001$ ) between treatments. **B** Thermal image of *A. pygmaeus* opening the elytra before taking off from the substrate captured by a thermal camera. White arrow indicates the location of the beetle.

We measured the body mass (XS205DU; Mettler-Toledo Ltd., Columbus, Ohio, USA) and body length (Euro-Cal Mark III; Sylvac SA, Yverdon-les-Bains, Switzerland) of each beetle immediately after the high-speed video recording (20 *A. dilutipes*, 29 *A. pygmaeus*). For those in which the elytra opening was recorded, we additionally measured the length and mass of the right elytron (20 *A. dilutipes*, 18 *A. pygmaeus*). On average, the larger species *A. dilutipes* was  $8.16 \pm 0.66$  mm long and  $26.33 \pm 7.64$  mg in weight with the elytron being  $6.66 \pm 0.56$  mm and  $899.5 \pm 248.3$   $\mu$ g while the smaller species *A. pygmaeus* was  $5.83 \pm 0.46$  mm long and  $13.25 \pm 11.60$  mg with the elytron being  $4.77 \pm 0.39$  mm and  $462 \pm 9.37$   $\mu$ g.

### High-speed video recording

To capture the movements of the beetle in the elytra opening and the beetle projection movement, we recorded the beetles from top view and lateral view, respectively. Since *Astraeus* beetles can flick in upside-down or right-side up positions, we also recorded the beetles in both starting positions for each phase. In total, 20 *A. dilutipes* and 29 *A. pygmaeus* were used for recording. Each individual was recorded one flicking event for each phase (elytra opening and body projection) and each positions (upside down and right-side up), totalling four videos. We excluded the videos where the beetles did not flick. For the elytra opening phase, we extracted movements of left and right elytra of the same individual from the same video. we recorded left and right elytra movement for 18 flicks in the upside-down position and 15 flicks in the right-side up position for *A. dilutipes* and 17 and 16 flicks for *A. pygmaeus*. For the body projection phase, we recorded 15 flicks in the upside-down position and 14 flicks in the right-side up position for *A. dilutipes* and 15 and 15 for *A. pygmaeus*.

At the beginning of each recording, the beetle was placed on a solid plastic substrate. The camera was placed vertically above the beetle to capture the elytra opening and laterally to capture body projection. We recorded using a high-speed video camera (NOVA S16, Photron, San Diego, California, USA) with a macro lens (100 mm; Canon Inc., Tokyo, Japan) and two external LED light sources (Zaila and Varsa; Nila Inc., Altadena, California, US). All the videos used in the analysis were recorded at 25,000 frames per second with a shutter speed of 10  $\mu$ s. A ruler with 1 mm scale and a 2.5 mm long reference paper was included in each top view and lateral view video, respectively, for distance calibration. The temporal and distance resolutions of the videos were  $4 \times 10^{-5}$  sec and  $1 \times 10^{-3}$  m, respectively. We recorded the top view (elytra opening) and the lateral view (body projection) in  $1024 \times 640$  pixel resolution. After the recording, the beetles were stored at  $-20^\circ\text{C}$  before further morphological examination.

To better understand the flicking behaviour, we recorded extra videos of the beetle flicking under various conditions. We first filmed a real time flick to show how fast the movement is to human eyes and demonstrated the beetle tucking its legs close to the body before flicking (Olympus OM-D E-M10 Mark III with a Olympus M.Zuiko 14–42 mm lens). We also recorded high-speed a video of an elytra opening prior to flight to compare the duration and elytra position with that of during the flick (Supplementary Movie 6). *Astraeus* beetles can open the elytra at different speeds, potentially for different purposes. It can be extremely fast at linear speeds of  $40.49 \pm 7.96$  m s $^{-1}$  (*A. pygmaeus*, 2<sup>nd</sup> elytron) to flick, or it can take >250 times longer ( $267.98 \pm 138.12$  m s $^{-1}$ ,  $N = 11$ ,  $n = 11$ , 8 *A. pygmaeus*, 3 *A. dilutipes*) to open the elytra prior to take-off. Other videos include close-up view of the upside-down flick to examine body arching prior the flick (Supplementary Movie 7), flicking when the elytra were removed partially and completely to test the effect of aerodynamics on body lifting (Supplementary Movie 8–10), flicking on a tiny platform to factor out physical contact with the elytra for body lifting (Supplementary Movie 11), hitting an object upon elytra opening or during the oscillation of the elytra to mimic the flick trajectory upon predation (Supplementary Movie 12–14), and sequential flicks to estimate the maximum flicks the beetles can perform in a row (Supplementary Movie 15).

### Kinematics of the elytra opening phase

To conduct a kinematic analysis of the flicks, we used Tracker (v.6.0.8; <http://physlets.org/tracker/>) to manually track the movement of the posterior tip of each elytron (right and left, separately). For the elytra opening phase, the elytra flick open then oscillate back and forth a few times. To capture the period of the highest velocity and acceleration, we tracked the initial opening of the elytra until the end of the first downstroke oscillation. For this period, we measured the displacement in radians of each elytron tip across every frame. From the same videos, we also measured the time for the elytron to reach the maximum displacement as the duration of the elytron opening.

For the elytra opening phase, we calculated 5 peak derivatives of elytral tips from the measured radians—angular velocity, angular acceleration, linear velocity, and linear acceleration, and perpendicular force generated. Specifically, we first calculated the angular velocity, angular acceleration of the elytron, and perpendicular force generated by the elytron tip using Eqs. (1) to (3)<sup>27</sup>,

$$\omega = \frac{d\phi}{dt} \quad (1)$$

$$\alpha = \frac{d\omega}{dt} \tag{2}$$

$$F_e = \frac{1}{3}M_e\alpha \tag{3}$$

where the angular velocity of the elytron  $\omega$  is the change of elytron tip in radians  $\phi$  over time  $t$ , the angular acceleration  $\alpha$  is the change of angular velocity of the elytron  $\omega$  over time  $t$ , and  $F_e$  is the perpendicular force generated by the elytron tip where  $M_e$  is the mass of the elytron.

To compare with other fast movement biological systems, we derived linear velocity,  $V_e$ , and linear acceleration,  $a_e$ , of the elytron tip from  $\omega$  and  $\alpha$  using Eqs. (4) and (5)<sup>37</sup>,

$$V_e = \omega r_e \tag{4}$$

$$a_e = \alpha r_e \tag{5}$$

where  $r_e$  is the length of the elytron.

We selected the maximum velocity, acceleration, and force for each flick to represent the peak performance of each elytron for subsequent analyses.

### Kinematics of the body projection phase

To understand the body kinematics at the initiation of the body projection, we used the same approach to track the movement of the most anterior and posterior tips of each beetle along the y-axis to derive the vertical displacement of the estimated body centre. We tracked the body propulsion in the first two elytra opening cycles (i.e., from the initiation of the elytra flicking open to the end of the second downstroke oscillation), which included the initiation of the lift off occurring at the beginning of the first downstroke and within the timeframe where the maximum kinematic values occurred. The tracking was conducted for every 3 frames instead of every frame to minimise noise from tracking. Because the beetles were placed parallel to the surface for the standardised measurement, the displacement in the x-axis was small and was not included in the measurement.

For the body projection phase, we calculated the 3 derivatives of the beetle body from the measured vertical displacement during the initial projection (elytra flicking open to the second downstroke) – vertical velocity of the body,  $V_b$ , vertical acceleration of the body,  $a_b$ , and vertical force generated by the body,  $F_b$ , using Eqs. (6) to (8),

$$V_b = \frac{dL}{dt} \tag{6}$$

$$a_b = \frac{dV_b}{dt} \tag{7}$$

$$F_b = M_b a_b \tag{8}$$

where  $L$  is the initial vertical displacement of the body and  $M_b$  is the body mass of the beetle.

We selected the maximum velocity, acceleration, and force for each flick to represent the peak performance of the beetle for subsequent analyses.

For the maximum height of the body projection, we used Tracker to measure the vertical distance from the estimated mass centre of the beetle (centre point between anterior and posterior tips) in the frame right before the projection to the frame in which the beetle reaches maximum height from the same video. There were four videos (1 for *A. dilutipes* and 3 for *A. pygmaeus*) where the beetles flicked higher than the top edge of the video frame and we were unable to measure the maximum height. These videos were excluded. To increase our sample size for this measurement, we added four videos filmed in wider views.

### Test for power amplification

To be a power amplified system, the minimum power required to generate the movement should be higher than the known maximum power any muscle can produce, i.e., the baseline of 200 W kg<sup>-110</sup>. To determine this, energy and power required for the movement can be calculated using Eqs. (9) and (10)<sup>10</sup>,

$$E_k = \frac{1}{2}M_e V_e^2 \tag{9}$$

$$P = \frac{E_k}{t_e} \tag{10}$$

where,  $E_k$  is the kinetic energy generated from the movement,  $P$  is the mechanical power output of the movement (energy per time unit), and  $t_e$  is the duration of the movement. Then power is divided by the mass of the muscles which may be involved in the movement to derive the maximum mass-specific power that can be compared to the baseline of 200 W kg<sup>-1</sup>.

Elytra are suggested to be controlled by mesothoracic muscles<sup>38</sup> but the protrusions (root) at anterior base of the elytra of *Astraeus* were observed extending into the prothorax. To account for uncertainty in muscles associated with elytral movement, we estimated the maximum power output of muscles conservatively by using the total muscle mass in both the prothorax and mesothorax as well as the time to reach the maximum radian in the calculation. To derive the mass of the fresh muscles for the above calculation, we anaesthetised four *A. pygmaeus* using carbon dioxide, quickly dissected the beetles, and removed and measured the mass of the muscles immediately before dehydration. We calculated muscle mass only for *A. pygmaeus* due to limited numbers of *A. dilutipes*.

### Escape temperature experiment

To test if the beetles initiated a flick at lower temperatures than typical escape behaviours such as flight, we performed a series of escape behavioural experiments. We measured the temperature at which the beetles flicked, walked and flew voluntarily. The temperature at which the beetle walked voluntarily was considered the lowest body temperature for functional movement. Additionally, we measured the temperature at which the beetle flicked in response to a simulated attack to determine if beetles can flick at a lower body temperature than voluntary flicks. Flicking was the only response to a simulated attack that we observed.

We recorded the trials with a thermal camera (model T540; Teledyne FLIR LLC, Wilsonville, Oregon, USA) and used FLIR Thermal Studio Pro (version 1.9.21.0) to extract body temperature data. In the first experiment, the beetles were placed on a cork board in the upside-down position because beetles often flick to right themselves. Once the beetle was placed, we heated the beetle using a tungsten halogen lamp (150 W HT150 tube, Arlec, Melbourne, Australia) ~ 30 cm above the beetle and recorded the temperature when the beetle flicked (voluntary flick). The trial was terminated if no flick occurred 5 min after warming commenced. The second experiment was similar to the first experiment, but the beetles were placed right-side up. We recorded both the temperature at which the beetles walked (moving steadily forward in one direction; voluntary walk) and flew (voluntary fly). The beetles usually walked and flew within ~13 min of the trial commencing. If flying did not occur 13 min after the warming commenced, the trial was terminated. Similarly, in the third experiment, we placed the beetles upside-down but on a wooden board without a heat source to prevent the body temperatures from increasing too quickly. During the experiment, we repeatedly pinched the beetle with forceps to mimic predator attacks and recorded the temperature at which the beetle flicked (triggered flick). The trial was terminated if no flick occurred 13 min after commencing warming for *A. pygmaeus* and 20 min for *A. dilutipes* due to their larger body size and slower heating rate. Trials terminated at the maximum trial duration without the occurrence of the target movements were excluded from subsequent analyses.

All the beetles were kept at 4°C and taken to a 17°C room where the temperature experiments were conducted immediately before each trial. We extracted body temperature at the starting point and when the behaviour (flick, walk, fly) was performed. Specifically, we circled the inner body outline of the focal beetle and used the average temperature to represent the body temperature of the beetle with emissivity set as 0.95<sup>39</sup>.

### Structure examination

To identify potential structures associated with the ultrafast flicking in *Astraeus* beetles, we examined the beetle structures internally and externally using both scanning electron microscopy (SEM) and micro-CT scanning.

For SEM samples, we dissected the beetle using a sharp razor blade, glued the sample on the aluminium SEM stubs with carbon adhesive tabs. After the samples (*A. pygmaeus*,  $n = 8$ ) were air dried (25 °C) for a week, we sputter coated them with a thin layer of gold-palladium using the Quorum QT5000 sputter coater and visualised the sample with the Hitachi TM4000 scanning electron microscope with a voltage of 5.0 kV.

For micro-CT samples, we first fixed the muscle tissues of the beetle samples (*A. dilutipes*,  $n = 2$ , *A. pygmaeus*,  $n = 2$ ) by placing them in 4% PFA for 24 h. Next, we rinsed the samples in PBS for 10 min for three times followed by immersing in iodine for 3 days. Finally, we rinsed the sample in PBS for 10 min for five times. Micro-CT scanning was performed with a phoenix nanotom m (Waygate Technologies) operated using xs control and phoenix datos|x acquisition software. Ten minute scans were conducted collecting 1199 projections through a full 360 degree rotation of the specimens. An energy of 60 kV and 200 microA was used with a Molybdenum target. Resolution was optimized to 3.75–4.25 (closed elytra) and 4–5.5 micrometer (open elytra) to capture full specimens in a single scan. Volume reconstruction of the micro-CT data was performed using the phoenix datos|x reconstruction software applying an inline median filter and ROI filter during reconstruction. Volume reconstructions were imported for Avizo3D Pro (Thermo Fisher Scientific) for analysis. Binary segmentations of elytra, collar and peg components were generated through manual selection and interpolation between keyframes selected in 2D cross-section. Surfaces were generated for each segmented component for visualization.

### Statistics and reproducibility

To test how kinematics of the elytra opening phase varied with position (upside-down/right-side up), species (*A. dilutipes*/*A. pygmaeus*), and opening order (first/second) we ran generalised linear mixed models (GLMM; lmer, R package lme4<sup>40</sup>;  $N = 36$ ,  $n = 132$ ). Six models were run, one for each kinematic variable: duration, angular velocity, angular acceleration, linear velocity, linear acceleration, and force. In all models, we included position, order, and species as the predictor variables. We also included the interaction of order and species since the asynchronism of elytra opening was more pronounced in *A. dilutipes* than *A. pygmaeus*. We also used GLMMs to test how position and species affected the flick of the whole beetle during the body projection phase ( $N = 31$ ,  $n = 59$ ). In these four models, we included position and species as the predictor variables with height, velocity, acceleration, or force as the response variable. Beetle ID was included as a random factor in all models to account for repeated measures (both elytra) on individuals.

To test if body temperature differed among behaviours, we ran a GLMM to compare the temperature among the four treatments (voluntary flick, voluntary walk, voluntary fly, triggered flick;  $N = 35$ ,  $n = 66$ ). In the model, we included the behaviour as the predictor variable and the starting body temperature as a covariate. We also included beetle ID and trial ID as random factors because we recorded the voluntary walk and voluntary fly temperature from the same beetle and 1–5 beetles were observed simultaneously within each trial. We only analysed data from *A. pygmaeus* due to the small sample size of *A. dilutipes*, however we present the data from four *A. dilutipes* individuals for different treatments in the results. All the statistical analyses were conducted in R (version 4.2.0<sup>41</sup>) and 0.05 was used for significance level.

### Reporting summary

Further information on research design is available in the Nature Portfolio Reporting Summary linked to this article.

### Data availability

All original data have been deposited at Dryad (<https://doi.org/10.5061/dryad.ht76hdrqd>)<sup>42</sup>. The original high-speed videos are available from the lead contact upon request.

### Code availability

Code for analyses and visualisation has been deposited at Dryad (<https://doi.org/10.5061/dryad.ht76hdrqd>)<sup>42</sup>.

Received: 22 August 2024; Accepted: 31 January 2025;

Published online: 13 February 2025

### References

- Cuthill, I. C. Camouflage. *J. Zool.* **308**, 75–92 (2019).
- Martín, J. & López, P. When to come out from a refuge: risk-sensitive and state-dependent decisions in an alpine lizard. *Behav. Ecol.* **10**, 487–492 (1999).
- Ruxton, G. D. et al. In *Avoiding Attack: The Evolutionary Ecology of Crypsis, Aposematism, and Mimicry* 2nd edn, Vol. 304 (OUP Oxford, 2018).
- Wang, L.-Y., Huang, W.-S., Tang, H.-C., Huang, L.-C. & Lin, C.-P. Too hard to swallow: a secret secondary defence of an aposematic insect. *J. Exp. Biol.* **221**, jeb172486 (2018).
- Wheatley, R., Angilletta, M. J. Jr, Niehaus, A. C. & Wilson, R. S. How fast should an animal run when escaping? an optimality model based on the trade-off between speed and accuracy. *Integr. Comp. Biol.* **55**, 1166–1175 (2015).
- Cooper, W. E. Jr & Sherbrooke, W. C. Strategic escape direction: orientation, turning, and escape trajectories of zebra-tailed lizards (*Callisaurus draconoides*). *Ethology* **122**, 542–551 (2016).
- Nadein, K., Kovalev, A. & Gorb, S. N. Jumping mechanism in the marsh beetles (Coleoptera: Scirtidae). *Scientific Reports* **12**, 15834 (2022).
- Ilton, M. et al. The principles of cascading power limits in small, fast biological and engineered systems. *Science* **360**, eaao1082 (2018).
- Burrows, M. Biomechanics: Frog hopper insects leap to new heights - an innovative leaping action propels these bugs to the top of the insect athletic league. *Nature* **424**, 509–509 (2003).
- Longo, S. J. et al. Beyond power amplification: latch-mediated spring actuation is an emerging framework for the study of diverse elastic systems. *J. Exp. Biol.* **222**, jeb197889 (2019).
- Patek, S. N., Korff, W. L. & Caldwell, R. L. Deadly strike mechanism of a mantis shrimp. *Nature* **428**, 819–820 (2004).
- Pringle, A., Patek, S. N., Fischer, M., Stolze, J. & Money, N. P. The captured launch of a ballistospore. *Mycologia* **97**, 866–871 (2005).
- Zaitsev, V. et al. A locust-inspired miniature jumping robot. *Bioinspir. Biomim.* **10**, 066012 (2015).
- Debray, A. Manipulators inspired by the tongue of the chameleon. *Bioinspir. Biomim.* **6**, 026002 (2011).
- Hyun, N. P. et al. Spring and latch dynamics can act as control pathways in ultrafast systems. *Bioinspir. Biomim.* **18**, 026002 (2023).
- Kuan, K. C., Chiu, C. I., Shih, M. C., Chi, K. J. & Li, H. F. Termite's twisted mandible presents past, powerful, and precise strikes. *Sci. Rep.* **10**, 9462 (2020).
- Yuan, Q. et al. Inside the coupling of ladybird beetle elytra: elastic setae can facilitate swift deployment. *J. Exp. Biol.* **225**, jeb244343 (2022).
- Frantsevich, L. Righting kinematics in beetles (Insecta: Coleoptera). *Arthropod Struct. Dev.* **33**, 221–235 (2004).

19. Nadein, K. & Betz, O. Jumping mechanisms and performance in beetles. I. Flea beetles (Coleoptera: Chrysomelidae: Alticini). *J. Exp. Biol.* **219**, 2015–2027 (2016).
20. Nadein, K. & Betz, O. Jumping mechanisms and performance in beetles. II. Weevils (Coleoptera: Curculionidae: Rhamphini). *Arthropod Struct. Dev.* **47**, 131–143 (2018).
21. Bolmin, O. et al. Latching of the click beetle (Coleoptera: Elateridae) thoracic hinge enabled by the morphology and mechanics of conformal structures. *J. Exp. Biol.* **222**, jeb196683 (2019).
22. Barker, S. Revision of the genus *Astraeus* Laporte & Gory (Coleoptera, Buprestidae). *Trans. R. Soc. S. Aust. Incorporated* **99**, 105–141 (1975).
23. Hawkeswood, T. J. Observations on some buprestidae (Coleoptera) from the blue mountains, N.S.W. *Aus. Zool.* **19**, 257–275 (1978).
24. Bartholomew, G. A. & Casey, T. M. Body temperature an oxygen consumption during rest and activity in relation to body size in some tropical beetles. *J. Thermal Biol.* **2**, 173–176 (1977).
25. Evans, M. The jump of the click beetle (Coleoptera, Elateridae)—a preliminary study. *J. Zool.* **167**, 319–336 (1972).
26. McHenry, M. J. et al. The comparative hydrodynamics of rapid rotation by predatory appendages. *J. Exp. Biol.* **219**, 3399–3411 (2016).
27. Patek, S. N., Baio, J. E., Fisher, B. L. & Suarez, A. V. Multifunctionality and mechanical origins: Ballistic jaw propulsion in trap-jaw ants. *Proc. Natl Acad. Sci. USA* **103**, 12787–12792 (2006).
28. Burrows, M. Jumping performance of froghopper insects. *J. Exp. Biol.* **209**, 4607 (2006).
29. Bolmin, O., McElrath, T., Wissa, A. & Alleyne, M. Scaling of jumping performance in click beetles (Coleoptera: Elateridae). *Integ. Comp. Biol.* **5**, 1227–1234 (2022).
30. Longo, S. J. et al. Geometric latches enable tuning of ultrafast, spring-propelled movements. *Integ. Exp. Biol.* **226**, jeb244363 (2023).
31. Sutton, G. P. et al. Dual spring force couples yield multifunctionality and ultrafast, precision rotation in tiny biomechanical systems. *J. Exp. Biol.* **225**, jeb244077 (2022).
32. Edwards, J., Whitaker, D., Klionsky, S. & Laskowski, M. J. A record-breaking pollen catapult. *Nature* **435**, 164–164 (2005).
33. Catchpole, C. K. & Slater, P. J. B. In *Bird song: Biological Themes and Variations* 2nd edn, Vol. 348 (Cambridge University Press, 2008).
34. Ribak, G. & Weihs, D. Jumping without using legs: the jump of the click-beetles (*Elateridae*) is morphologically constrained. *PLoS ONE* **6**, e20871 (2011).
35. Evans, M. The jump of the click beetle (Coleoptera: Elateridae)—energetics and mechanics. *J. Zool.* **169**, 181–194 (1973).
36. Slipinski, A. & Lawrence, J. *Australian Beetles Volume 2: Archostemata, Myxophaga, Adepaga, Polyphaga (part)* Vol. 792 (CSIRO Publishing, 2019).
37. Longo, S. J. et al. Snaps of a tiny amphipod push the boundary of ultrafast, repeatable movement. *Curr. Biol.* **31**, R116–R117 (2021).
38. Frantsevich, L. Experimental evidence on actuation and performance of the elytron-to-body articulation in a diving beetle, *Cybister laterimarginalis* (Coleoptera, Dytiscidae). *J. Insect Physiol.* **58**, 1650–1662 (2012).
39. Gallego, B., Verdu, J. R., Carrascal, L. M. & Lobo, J. M. A protocol for analysing thermal stress in insects using infrared thermography. *J. Thermal Biol.* **56**, 113–121 (2016).
40. Bates, D., Machler, M., Bolker, B. M. & Walker, S. C. Fitting linear mixed-effects models using lme4. *J. Stat. Softw.* **67**, 1–48 (2015).
41. *R: A Language and Environment for Statistical Computing.* <https://www.r-project.org/> (2018).
42. Wang, L.-Y., Stuart-Fox, D., Lee, K.-H., Black, J. & Franklin, A. M. *Dataset for: A New Ultrafast Movement Enables Escape at Low Temperature.* <https://datadryad.org/stash/> (2025).

## Acknowledgements

We thank Allen Sundholm and Geoff Walker for providing location information for the beetles, Katrina Rankin for the assistance with field collection, Anita Huang for accommodation during the fieldwork, and Prof. Florian Muijres and Prof. Johan van Leeuwen for insightful discussion. We also thank The University of Melbourne for funding the high-speed camera, the Biological Imaging Platform for the access to the high-speed camera and the scanning electron microscopy, and the Melbourne TrACEES (Trace Analysis for Chemical, Earth and Environmental Science) Platform for access to the Phoenix Nanotom M micro-CT scanner. This study was supported by Jasper Loftus-Hills Memorial Scholarship to L.-Y.W., a Melbourne Postdoctoral Fellowship to A.M.F., and Australian Research Council Fellowship (FT180100216) to D.S.-F.

## Author contributions

L.-Y.W. contributed to conceptualisation, methodology, field collection, data collection, formal analysis, writing - original draft, visualisation, and funding acquisition. D.S.-F. contributed to conceptualisation, methodology, resources, writing - review & editing, supervision, and funding acquisition. K.-H.L. contributed to field collection and writing - review & editing. J.B. contributed to data collection and writing - review & editing. A.M.F. contributed to conceptualisation, methodology, resources, writing - review & editing, and supervision.

## Competing interests

The authors declare no competing interests.

## Additional information

**Supplementary information** The online version contains supplementary material available at <https://doi.org/10.1038/s42003-025-07650-7>.

**Correspondence** and requests for materials should be addressed to Lu-Yi Wang.

**Peer review information** *Communications Biology* thanks Konstantin Nadein, Ophelia Bolmin, and the other, anonymous, reviewer for their contribution to the peer review of this work. Primary Handling Editor: Jasmine Pan. A peer review file is available

**Reprints and permissions information** is available at <http://www.nature.com/reprints>

**Publisher's note** Springer Nature remains neutral with regard to jurisdictional claims in published maps and institutional affiliations.

**Open Access** This article is licensed under a Creative Commons Attribution-NonCommercial-NoDerivatives 4.0 International License, which permits any non-commercial use, sharing, distribution and reproduction in any medium or format, as long as you give appropriate credit to the original author(s) and the source, provide a link to the Creative Commons licence, and indicate if you modified the licensed material. You do not have permission under this licence to share adapted material derived from this article or parts of it. The images or other third party material in this article are included in the article's Creative Commons licence, unless indicated otherwise in a credit line to the material. If material is not included in the article's Creative Commons licence and your intended use is not permitted by statutory regulation or exceeds the permitted use, you will need to obtain permission directly from the copyright holder. To view a copy of this licence, visit <http://creativecommons.org/licenses/by-nc-nd/4.0/>.

© The Author(s) 2025